ISSN: 2414-1895 DOI: 10.6919/ICJE.202204_8(4).0005

Reconstruction of Limited-angle EMT Images based on SB Algorithm

Yalin Yao

Shanghai Maritime University, Shanghai, China

Abstract

For limited projection data, EMT images reconstructed by traditional algorithms have serious artifacts and obvious noise. Based on this situation, this paper deduces and establishes the EMT image reconstruction model. The EMT image reconstruction problem under limited angle is analyzed, the L_1regularization solution strategy of the problem is given, and the split bregamn algorithm of the reconstruction model is proposed. Simulation experiments show that for the data with limited angle, split bregamn algorithm can be compared with the traditional Tikhonov algorithm and Landweber algorithm. Split bregamn algorithm has better subjective reconstruction effect, the average image error is reduced by 30.4%, and the quality of image reconstruction is effectively improved.

Keywords

EMT Image Reconstruction; Limited Angle; Split Bregamn; L_1 Regularization.

1. Introduction

Electromagnetic tomography [1] (Electrical Induction Tomography, EMT) is a technology based on the principle of electromagnetic induction and can reconstruct the distribution of electrical characteristics of the measured object. Due to the advantages of online detection, fast response, and visualization, it is widely used in metallurgy, rail transit, medicine and other fields [2-4]. However, in actual measurement, due to the constraints of equipment and location factors, the obtained data is not complete. In 2006, Donoho [5], Candes [6] and Zhang Xiaodong [7] proposed a new information acquisition theory: compression Sensing (compressed sensing.CS) theory. CS theory points out that if the signal is sparse in a certain transform domain, only a small number of signal samples are needed, and the original signal can be accurately recovered by solving an optimization problem. Inspired by CS theory, the literature [8-9] made a breakthrough using the sparse prior knowledge of total variation minimization (TVM) of images, combined with POCS (projection onto convex sets, POCS) method and adaptive The adaptive steepest descent (ASD) algorithm proposed ASD-POCS, but the robustness and speed of the ASD-POCS algorithm were poor. Wang Linyuan [10] and others studied the sparse signal recovery theory in the cone beam limited The preliminary application in angular CT image reconstruction has opened up a new direction for the development of this field. Lu Xiaoqiang [11] and others studied a finite-angle CT reconstruction algorithm based on multiplicative regularization. This algorithm has the advantages of the total variation method and can adaptively adjust the regularization parameters in the iterative process, which overcomes the TV minimization. The weight parameters of the function must be determined through a large number of experiments. Zhang Yulin et al. [12] studied the general CT image reconstruction algorithm based on Split Bregman, mainly considering that it can effectively remove the noise in the energy spectrum channel, meet the needs of object material distinction, and did not consider the artifact factor. Kang Hui et al. [13] studied the CT image reconstruction algorithm based on Bregman iteration, and achieved satisfactory results, but they did not consider the "split" method for reconstruction, and its projection

ISSN: 2414-1895 DOI: 10.6919/ICJE.202204_8(4).0005

was a non-finite angle projection. Gou et al. [14] used the Split Bregman algorithm for the iterative reconstruction of half-coverage projection CT, which did not involve the image reconstruction problem in the case of limited angles. Guo Jingyu et al. [15] proposed that the average value of various uniform tissues in the prior image was introduced into the reconstructed image objective function as prior information, which greatly reduced the artifacts and deformation of the reconstructed image. The effect of finite angle reconstruction for noisy situations is not considered.

The above literatures are mainly based on CS theory to carry out the method research on finite angle reconstruction of CT images, which can also be used for reference in EMT image reconstruction. In this paper, we will try to learn from the idea of literature [16], combine algebraic iterative reconstruction and L_1 $r$egularization as the prior constraint of EMT finite-angle reconstruction, and based on the Split Bregman algorithm, study the finite-angle EMT reconstruction problem from the perspective of sparse optimization, and plan to carry out The simulation verification of the proposed algorithm and the comparison with Tikhonov algorithm [17] and Landweber algorithm [18] are expected to improve the reconstruction effect of limited-angle EMT images.

2. EMT Image Reconstruction and Sensor Array Structure

2.1 The Theoretical Basis of EMT

The mathematical model of EMT image reconstruction is shown in formula (1):

$$v = F(\mu) \tag{1}$$

In the formula: μ represents the magnetic permeability distribution; v represents the measurement value of the detection coil; F represents the nonlinear function determined by the system. Since it cannot be determined whether the measured value v is included in the value range of F, it is impossible to directly solve equation (1), so equation (1) can be expanded by the second-order Taylor formula as:

$$v = F(\mu_0) + \frac{\partial F}{\partial \mu}|_{\mu_0}(\mu - \mu_0) + o(||\mu - \mu_0||) \tag{2}$$

In the formula: $\frac{\partial F}{\partial \mu}$ represents the sensitivity matrix, that is, the change rate of the detected value on the induction coil caused by the change of the magnetic permeability of the measured field; μ_0 represents the original magnetic permeability distribution, that is, the magnetic permeability distribution in the empty field; μ is the magnetic permeability distribution to be measured. When the change of the permeability distribution of the measured object field is sufficiently small, equation (2) can be transformed into:

$$v - F(\mu_0) = \frac{\partial F}{\partial \mu}|_{\mu_0}(\mu - \mu_0) \tag{3}$$

Then the measured object field is discretized, then for an EMT system with m independent measurement values and n finite elements, it can be expressed as the matrix form shown in equation(4):

$$U_{m\times 1} = S_{m\times n} G_{n\times 1} \tag{4}$$

In the formula: U is the data vector of measurement; S is the sensitivity matrix; G is the pixel point of the permeability distribution.

ISSN: 2414-1895 DOI: 10.6919/ICJE.202204_8(4).0005

2.2 Common Image Reconstruction Algorithms in EMT

According to the prior information sensitivity matrix S and the measured voltage column vector U to solve Equation (4), the measured metal conductivity distribution matrix representing the crack position and size information is obtained, and the catalyst distribution is represented in the form of an image to solve ,the image reconstruction. Because the measured data is limited, and the number of pixels in the measured area is far more than the amount of detected data, that is, the number of unknowns in the equation is far more than the number of equations, the solution of equation (4) is ill-conditioned. To solve this ill-conditioned equation, common methods include Linear Back Projection (LBP) algorithm, Landweber iterative algorithm, and Tikhonov regularization algorithm.

2.3 Sensor Array Structure and EMT System Parameter Setting

In this paper, the model of the sensor array that does not completely surround the "C" type is used, all coils are evenly distributed around the shield layer, and the coil axis is perpendicular to the shield layer.

In Figure 1, the diameter of the circular imaging area is 100mm, the size and shape of the eight coils are the same, the inner diameter of the coil is 2mm, the outer diameter is 38mm, the coil height is 5mm, and the number of turns is 200.

This sensor still uses the traditional single-coil excitation mode: in the simulation process, first excite excitation coil 1, record the magnetic induction intensity from sensor point 2 to measurement point 8, and then follow this operation to sequentially excite coil 2 to coil 8 and record Corresponding to the magnetic induction intensity value of the detection point group, 8×7=56 independent magnetic induction intensity measurement values can be obtained, and the conductivity distribution in the sensor range can be obtained.

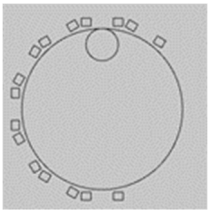

Figure 1. "C" type sensor array model

3. EMT Image Reconstruction based on Split Bregman Algorithm

3.1 Bregman Distance

If given a differentiable convex function J(u): $R^n \to R$ and define the distance between two points μ and v in R^n as:

$$D_J^p(u,v) = J(u) - J(v) - < p, u - v >. \tag{5}$$

Where: P is the subgradient of function J at point V. Obviously, this distance is not a distance in the usual sense. But it can be used to measure how close point u is to point v. When the differentiable convex function $J(u)$ is a Bregman function, its corresponding distance $D_J^p(u,v)$is called the Bregman distance. Due to the convexity of the function J(u), for any point ω on the line connecting u and v, there are $D_J^p(u,v) \geq 0$ and $D_J^p\ (u,v) \geq D_J^p\ (w\ ,v)$. Considering the convex energy functional, J and L belong to the R^n space and have $minL(u)0$, then the corresponding unconstrained minimization problem is:

$$\min_u \left| \phi(u) \right| + \mu L(u) \tag{6}$$

ISSN: 2414-1895 DOI: 10.6919/ICJE.202204_8(4).0005

In the formula: $|\emptyset(u)|$ means to solve the L_1norm; $L(u)$ is the constraint part of the problem, which is often in the form of the L_2 norm; μ is called the regularization parameter, which is used to balance the relative sizes of the two parts.

3.2 Bregman Iteration

In many applications of image processing, the problem to be solved is often the L_1 regularization optimization problem. According to formula (6), for the EMT image reconstruction problem to be studied, it can be expressed as formula (7).

$$minD_J^p(u,u^k)s.t.SG = U \tag{7}$$

In order to solve Equation (7) conveniently, it needs to be converted into an equivalent unconstrained representation. Using the penalty function form to describe, Equation (7) can be further transformed into Equation (8):

$$u^{k+1}=argminD_J^p(u,u^k)+\frac{\mu}{2}||SG-U^k||_2^2 \tag{8}$$

where μ is the balance regularization parameter between fidelity and coefficient conditions, and Equation (8) is the problem to be solved in this paper. Equation (5) is brought into Equation (8), and the optimization conditions are applied, Deformation results in the basic Bregman iterative model. As shown in formula (9).

$$\begin{cases} u^{k+1}=\underset{f}{argminJ}(u)+\frac{\mu}{2}||SG-U^k||_2^2 \\ U^{k+1}=U^k+U-SG^k \end{cases} \tag{9}$$

in the formula: $J(u)=||u||1.$

3.3 Split Bregman Algorithm Solving

The L_1regularization problem is solved by applying the Split Bregman iterative method as follows. In this method, considering the energy functional L_1part and the energy functional L_2part in Eq. (6) respectively, there is Eq. (10):

$$\min_{u,d}|d|+L(u)\ s.t.d=\phi(u). \tag{10}$$

Equation (10) needs to be transformed into the unconstrained problem Equation (11):

$$\min_{u,d}|d|+L(u)+\frac{\mu}{2}\|d-\phi(u)\|_2^2 \tag{11}$$

Suppose $J(u,d)=|d|+L(u)$, and define $A(u,d)=d-\phi(u)$, then formula (11) is the specific application of formula (8), in order to strengthen the constraint condition, transform the Bregman iteration formula into a two-parameter form, as shown in formula (12).

ISSN: 2414-1895 DOI: 10.6919/ICJE.202204_8(4).0005

$$\begin{cases} (u^{k+1}, d^{k+1}) = \underset{u,d}{argmin} D_J^p(u, u^k, d, d^k) + \frac{\mu}{2}\|d - \phi(u)\|_2^2 = \underset{u,d}{argmin} J(u,d) - <p_u^k, u - u^k> - <p_d^k, \\ d - d^k> + \frac{\mu}{2}\|d - \phi(u)\|_2^2, \\ p_u^{k+1} = p_u^k - \mu(\nabla\phi)^T(\phi u^{k+1} - d^{k+1}), \\ p_d^{K+1} = p_d^k - \mu(d^{k+1} - \phi u^{k+1}). \end{cases} \tag{12}$$

Applying the simplified form of Equation (9), the Split Bregman iteration (13) of the two terms can be obtained.

$$\begin{cases} (u^{k+1}, d^{k+1}) = \underset{u,d}{argmin} |d| + L(u) + \frac{\mu}{2}\|d - \phi(u) - U^k\|_2^2, \\ U^{k+1} = U^k + (\phi(u^{k+1}) - d^{k+1}). \end{cases} \tag{13}$$

In order to effectively achieve the minimization effect, the functional described by equation (13) is divided into $L_1$and L_2 parts, which are minimized for the variables u and d respectively. In order to solve the above problem, it is necessary to pass equations (14) and (15) to solve.

$$u^{k+1} = \underset{u}{argmin} L(u) + \frac{\mu}{2}\|d^k - \phi(u) - U^k\|_2^2, \tag{14}$$

$$d^{k+1} = \underset{d}{argmin} |d| + \frac{\mu}{2}\|d - \phi(u^{k+1}) - U^k\|_2^2 \tag{15}$$

4. Analysis of Simulation Results

Table 1. (a)distribution of catalysts with particle size of 4mm

number	Simulation model	Tikhonov	Landweber	Split Bregman
1	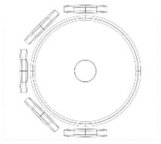	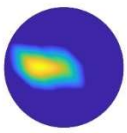		
2	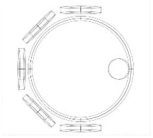	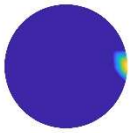		
3		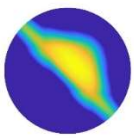	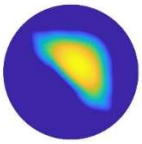	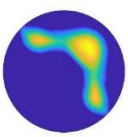

ISSN: 2414-1895 DOI: 10.6919/ICJE.202204_8(4).0005

In order to verify the effectiveness of the algorithm, a simulation experiment is carried out in COMSOL Multiphysics, and the Tikhonov algorithm, the Landweber iteration method and the Split Bregman algorithm are used for imaging respectively.

This paper studies the distribution of 5mm10mm. The specific location distribution and imaging results are shown in Figure 3. The simulation models are numbered 1-6 from top to bottom, and the small circles in the simulation model plan represent spherical catalysts.

Observing Figure 3, it can be seen that the position distribution of the catalyst can be detected based on three algorithms. However, intuitively, whether it is a distribution with a particle size of 4 mm or a particle size of 8 mm, the imaging results of the Split Bregman algorithm have the least artifacts,and the restoration of the position and shape of the catalyst is also the best, indicating that the Split Bregman algorithm has better edge processing capability than the other two algorithms, which is convenient for subsequent monitoring of the shape and quality of the catalyst.

Table 2. (b)distribution of catalysts with particle size of 8mm

number	Simulation model	Tikhonov	Landweber	Split Bregman
4		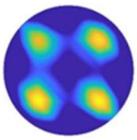	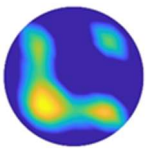	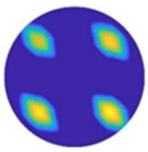
5		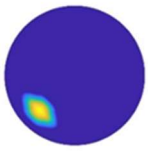	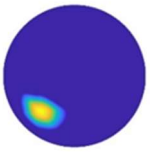	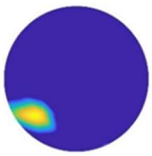
6	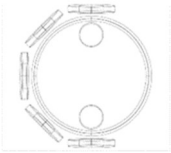	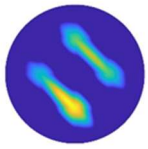	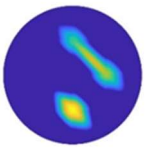	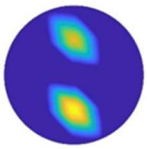

In the reconstructed image in Figure 3, the orange-yellow part represents the area with catalyst, the dark-blue part represents the catalyst-free area, and the light-blue part is due to noise and artifacts introduced by the algorithm. In order to quantitatively evaluate the performance of the algorithm, this paper uses the relative error of the image to evaluate the relative error of the image [19] (Relative Error, RE) to evaluate the imaging quality. The calculation formula is as follows:

$$RE = \frac{||G^* - G||}{||G||} \tag{16}$$

In formula (13): G^* is the calculated distribution of conductivity, and G represents the actual distribution of conductivity.

ISSN: 2414-1895 DOI: 10.6919/ICJE.202204_8(4).0005

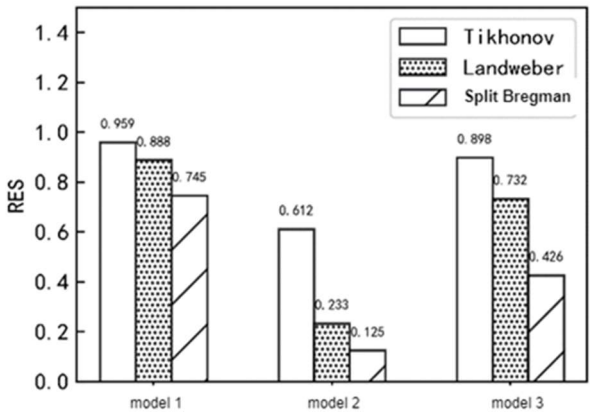

Figure 2. RE value of defect distribution with a particle size of 4 mm

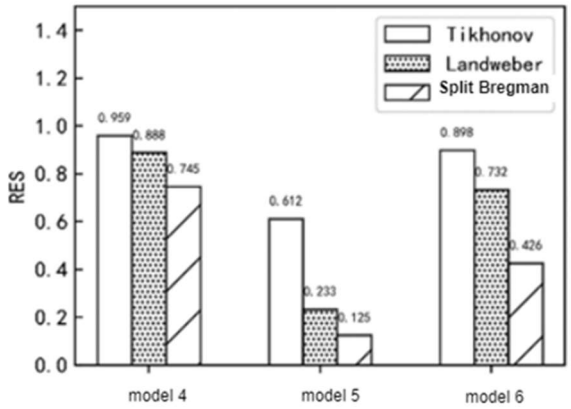

Figure 3. RE value of defect distribution with a particle size of 8 mm

The comparison of the relative errors of the images of each model under the three reconstruction algorithms is shown in Figure 4. Compared with the other two algorithms, the images reconstructed by the Split Bregman algorithm have smaller relative errors, which proves that the CoSaMP algorithm has a better imaging quality. superiority. Table 2 shows the imaging time required by the three algorithms to obtain the imaging results in Figure 4. It can be seen from the table that the Landweber algorithm requires the longest imaging time due to the need for multiple iterations, while the Split Bregman algorithm takes the longest time in the iterative process. Discard irrelevant atoms to improve the convergence speed, so the required iteration time is shorter, and the i maging speed is the fastest among the three algorithms.

Table 3. Imaging Time of Different Algorithms

Number	Tikhonov	Landweber	Split Bregman
Model 1	2.15	3.24	1.25
Model 2	2.11	3.35	1.26
Model 3	2.33	3.25	1.73
Model 4	2.26	3.21	1.46
Model 5	2.35	3.21	1.43
Model 6	2.33	3.19	1.52

ISSN: 2414-1895 DOI: 10.6919/ICJE.202204_8(4).0005

5. Conclusion

In this paper, the imaging of EM conclusion T technology under limited angle is studied. Due to the constraints of equipment and location, the obtained data is not complete. The Split Bregman algorithm is used for imaging, and the simulation experiment performed on Comsol software is used. Based on the Split Bregman algorithm, the imaging of EMT at a limited angle is realized. The simulation results show that compared with the traditional Tikhonov regularization algorithm and Landweber iterative algorithm, the imaging results of the Split Bregman algorithm have fewer artifacts, indicating that the algorithm has better performance. .Compared with the other two algorithms, the Split Bregman algorithm converges faster than the other two algorithms, which can effectively improve the accuracy and speed of detection. The next step will be to further optimize the imaging algorithm under the limited angle to improve the detection quality and speed.

References

[1] Wang Shaojing, Wang Fenghua, Zhou Dongxu, et al. Anomaly detection of grounding grid conductors based on electromagnetic tomography [J/OL]. Electrical Measurement and Instrumentation: 1-9 [2020-12-04].

[2] Ma L, Hunt A, Soleimani M. Experimental evaluation of conductive flow imaging using magnetic induction tomography[J]. International Journal of Multiphase Flow, 2015, 72: 198-209.

[3] Wang C, Liu Z, Huo J, et al. Research on defect detection method for high-speed train hollow shaft by electromagnetic tomography[J]. Foreign Electronic Measurement Technology,2020.

[4] Delussi Marianna,Nazzaro Virgilio,Ricci Katia,de Tommaso Marina. EEG Functional Connectivity and Cognitive Variables in Premanifest and Manifest Huntington's Disease: EEG Low-Resolution Brain Electromagnetic Tomography (LORETA) Study [J]. Frontiers in Physiology,2020,{4}{5}.

[5] David L. Donoho. Compressed sensing.[J]. IEEE Trans. Information Theory, 2006, 52(4) : 1289-1306.

[6] Emmanuel J. Candès. The restricted isometry property and its implications for compressed sensing[J]. Comptes rendus -Mathématique, 2008, 346(9) : 589-592.

[7] Zhang Xiaodong, Dong Weiguang, Tang Min'an.Research on road traffic image processing and reconstruction algorithm based on compressed sensing[J].Journal of Lanzhou Jiaotong University,2016, 35(04):50-55.

[8] Sidky Emil Y. and Kao ChienMin and Pan Xiaochuan. Accurate image reconstruction in CT from projection data taken at few-views[J]. 2006, 6142 : 614229-614229-7.

[9] Emil Y Sidky and Xiaochuan Pan. Image reconstruction in circular cone-beam computed tomography by constrained, total-variation minimization[J]. Physics in Medicine and Biology, 2008, 53(17) : 4777-807.

[10] Wang Linyuan, Li Lei, Yan Bin, Jiang Chengshun, Wang Haoyu, Bao Shanglian.Application of Sparse Signal Recovery Theory in CT Image Reconstruction[J].CT Theory and Application Research,2009, 18 (03):22-29.

[11] Lu Xiaoqiang, Sun Yi. Finite Angle CT Reconstruction Algorithm Based on Multiplicative Regularization[J]. Journal of Optics, 2010,30(05):1285-1290.

[12] Zhang Yulin, Kong Huihua, Pan Jinxiao, Han Yan.Reconstruction of energy spectrum computed tomography images based on Split-Bregman algorithm[J].Acta Optics,2017,37(04):153-161.

[13] Kang Hui, Gao Hongxia, Hu Yueming, Guo Qiwei. CT Image Reconstruction Algorithm Based on Bregman Iteration[J].Acta Automata,2013,39(09):1570-1575.

[14] Gou J Dong H. CT image reconstruction of half-covered projection with fewer iterations based on SB-TVM[J]. INSIGHT, 2016, 58(7) : 373-379.

[15] Guo Jingyu, Qi Hongliang, Yuan Yuan, Zhou Linghong. A limited-angle CT image reconstruction algorithm with prior image constraints [J]. Nuclear Electronics and Detection Technology, 2014,34(12): 1421-1424.

[16] Zhao Zengfang. Split Bregman Method for Image Decomposition[D]. Qingdao University, 2011.

[17] Liu Xianglong, Liu Ze, Zhu Sheng. Modified Landweber Iterative Algorithm in Electromagnetic Tomography Image Reconstruction [J]. Chinese Journal of Electrical Engineering, 2019, 39(13).

ISSN: 2414-1895 DOI: 10.6919/ICJE.202204_8(4).0005

[18] Wen Limei, Zhou Miaomiao, Li Ming, et al. Improved Tikhonov Regularized Image Reconstruction Algorithm[J]. Journal of Metrology, 2018(5):679-683.

[19] WANG Q, ZHANG J W, ZHANG R H, XUE F J, LI X Y. Research on electromagnetic imaging of metal defects based on the Bayesian statistical model [J]. Chinese Journal of Scientific Instrument, 2020,41(01) : 47-55.